SUPPLEMENTAL MATERIAL

Detailed Methods

Mice

All mice were housed and bred in specific pathogen–free conditions in the Animal Research Facility at the San Francisco Veterans Affairs Medical Center. All animal experiments were approved by the Institutional Animal Care and Use Committee at the VA Medical Center. WT C57BL/6, *Ldlr*$^{-/-}$ (B6.129S7-*Ldlr*^{tm1Her}/J) and *Apoe*$^{-/-}$ (B6.129P2-*Apoe*^{tm1Unc}/J) mice (3-4 weeks old) were purchased from The Jackson Laboratory and fed with a rodent chow diet containing 4.0% fat (Harlan Teklad, 2916), or high fat diet (21% fat, 1.5% cholesterol, Research Diets, D12079B). *Apoe*$^{-/-}$*Ldlr*$^{-/-}$ and *Apoe*$^{h/h}$*Ldlr*$^{-/-}$ mice, established as previously described,[1] were fed a rodent chow diet of equal nutritional value containing 4.0% fat (Harlan Teklad, 2916) and 9.0% fat (Harlan Teklad, 2919) respectively.

Cells

Bone marrow cells from both the tibias and femurs were harvested from euthanized mice by inserting needles into the bone and washing with RPMI-1640 (UCSF Cell Culture Facility) and filtered through a 70 μM cell strainer (BD Biosciences). Peripheral blood was drawn from anesthetized mice via retro-orbital puncture with heparinized micro-hematocrit capillary tubes (Fisher Scientific). Resident peritoneal macrophages were harvested from mice with 10 ml RPMI 1640 and purified by adherence to tissue culture plastic for 2 hours. Spleens were removed, homogenized gently using plungers, and then filtered through a 70μM cell strainer. Red blood cells were lysed with ACK lysis buffer. Aortic single cells were prepared from *Apoe*$^{-/-}$*Ldlr*$^{-/-}$ and *Apoe*$^{h/h}$*Ldlr*$^{-/-}$ mice as previously described.[2] In brief, after careful removal of the perivascular fat and cardiac tissue using micro-scissors under a dissecting microscope, single cell suspensions from aortic segments, including the aortic arch and thoracic aorta were prepared by incubation with an enzyme mixture containing 675 U/ml collagenase I, 187.5 U/ml collagenase XI, 90 U/ml hyaluronidase, and 90 U/ml DNase I (all from Sigma-Aldrich) in Hank's balanced salt solution for 60 min at 37 °C. The resulting single-cell suspensions were washed with Stain Buffer (BD Biosciences) for flow cytometric analysis and sorting or washed with the designed cell culture medium for the *in vitro* studies.

Cell culture

Bone marrow–derived macrophages (BMDM) from WT and *Apoe*$^{-/-}$ mice were prepared as adherent cultures using recombinant mouse M-CSF (30 ng/ml, Peprotech). For ectopic expression of apoE in *Apoe*$^{-/-}$ BMDMs and Ly-6C^{high} monocytes, the cells were cultured in Opti-MEM (Life Technologies) and transiently transfected with mouse *Apoe* cDNA clone or control expression plasmids (Origene) using Lipofectamine 2000 (Life Technologies) as per the manufacturer's instructions. For RNA interference experiments, scramble control or apoE siRNA (50 nM, Life Technologies) or PU.1 siRNA (100 nM, GE Dharmacon) [3, 4] were transfected into BMDM or Ly-6C^{high} monocytes or BMDM using Lipofectamine RNAiMAX Reagent (Invitrogen) according to the manufacturer's protocol. At 24 hrs or 48 hrs post transfection, total RNA was extracted and used for qPCR analysis. Target gene knockdown efficiency was validated by qPCR.

Flow cytometry

Fluorescent dye–labeled anti-CD11b (M1/70), anti-F4/80 (BM8), anti-CD19 (1D3), anti-B220 (RA3-6B2), anti-NK1.1 (PK136), anti-Ly-6G (RB6-8C5), anti-Ly-6G (1A8), anti-Ly-6C (AL-21),

anti-CD115 (AFS98), anti-CD11c (HL3), anti-TCR-β (H57-597), and anti-CD3 (145-2C11) antibodies were purchased from BD Biosciences, eBioscience or BioLegend. The gating strategy to identify Ly-6C^{high} monocytes (CD11b^{+}CD115^{high}Ly-6C^{high}), Ly-6C^{low} monocytes (CD11b^{+}CD115^{high}Ly-6C^{low}), neutrophils (SSC^{high}CD11b^{+}Ly-6G^{+}), CD8α^{+} DCs (CD11c^{high}CD8α^{+}), CD11b^{+} DCs (CD11c^{high}CD11b^{+}), pDCs (CD11c^{int}CD11b^{-}B220^{+}Ly-6C^{+}), B cells (B220^{+}CD19^{+}) and T cells (CD3^{+}TCR-β^{+}) are shown in **Online Figure VI**, **V** and **VI**.

Multicolor flow cytometry was performed using standard procedures. Briefly, 1 × 10^{6} cells were incubated with anti-CD16/CD32 (2.4G2; UCSF Cell Culture Facility) in 100 µl BD Stain Buffer (DPBS with 0.2% BSA) for 10 min. Without washing, the cells were incubated at 4 °C with combinations of antibodies for 30 min, washed and resuspended in BD Stain Buffer. CountBright Beads (Invitrogen) were added to aortic samples before acquisition to determine the absolute cell numbers.

Intracellular TNF-α staining was performed as previously reported. [5] Briefly, spleen cells were stimulated for 4 h with 50 ng/ml LPS (serotype O55:B5) (Sigma) in the presence of Golgi-plug (BD Biosciences). After stimulation, cells were first stained with cell-surface marker antibodies, fixed and permeabilized with a Cytofix/Cytoperm kit (BD Biosciences), and then stained with APC-conjugated rat anti-mouse TNF-α antibody (BD Biosciences). For intracellular ApoE staining, freshly isolated bone marrow cells or peritoneal cells were first stained with monocyte or macrophage cell-surface marker antibodies, fixed and permeabilized with a Cytofix/Cytoperm kit (BD Biosciences), and then stained with rabbit anti-mouse ApoE antibody (Meridian Life Science, K23100R), followed by a R-PE-conjugated goat anti-rabbit IgG (H+L) antibody (Life Technologies). ApoE antibody was validated for specificity as in **Online Figure VII**.

For analysis of phosphorylated p65, total blood leukocytes and peritoneal cells were stimulated with 100 ng/mL LPS for 30 min and 15 min respectively, fixed with Cytofix Fixation Buffer, permeabilized with chilled Perm Buffer II or Perm Buffer III (BD Biosciences), and then stained with Alexa Fluor 488 or Alexa Fluor 647-conjugated phospho-NF-κB p65 (Ser536) antibody (93H1; Cell Signaling) and the antibodies specific for surface markers identifying macrophages and monocytes. For PU.1 staining, peritoneal cells or BMDM was first stained with PerCP-Cy5.5-anti-CD11b and FITC-anti-F4/80 antibodies, fixed and permeabilized with a Foxp3/Transcription Factor Staining Buffer Set (eBioscience, 00-5523), and then stained with a Alexa Fluor 647 Conjugated rabbit anti-mouse PU.1 (9G7) mAb (Cell Signaling Technology).

Data were acquired on a LSR II flow cytometer using the FACS Diva software or Accuri C6 cytometer using CFlow Plus software (all instruments and software from BD Biosciences) and analyzed using FlowJo (TreeStar Inc.). All cell sorting was performed on FACS ARIA II or III sorters (Becton Dickinson) at the UCSF flow cytometry core facility.

Quantitative Real-Time PCR

Total RNA was extracted from flow cytometry-sorted cells or macrophages using mirVana miRNA Isolation Kit (Life Technologies) according to the manufacturer's protocol. MiR-146a expression was measured with TaqMan miRNA assays (Applied Biosystems) according to the vendor protocol and normalized by sno202 snRNA levels. To quantitate cellular levels of the NF-κB–related miRNAs, total RNA was polyadenylated and reverse transcribed by using the NCode miRNA first-strand synthesis kit (Invitrogen) according to the manufacturer's instructions. The resulting cDNA was subjected to qRT-PCR using the NCode universal reverse primer (Invitrogen) in conjunction with a sequence-specific forward primer for individual microRNA. Similarly, sno202 snRNA was quantified using the NCode universal reverse primer and a sno202-specific primer.

To quantitate mRNA, the cDNA was synthesized with total RNA and iScript cDNA Synthesis Kit (Bio-Rad) according to the manufacturer's protocol. The expression of genes encoding apoE (Mm01307193_g1), TNF-α (Mm00443260_g1), IL-6 (Mm00446190_m1), IRAK1 (Mm01193538_m1), TRAF6 (Mm00493836_m1), pri-miR-146a (Mm03306349_pri), PU.1 (Mm00488142_m1), β-2 microglobulin (β2m, Mm00437762_m1) and Rn18s (Mm03928990_g1) was assessed by real-time PCR with mouse TaqMan Gene Expression Assays (Life Technologies); results were normalized to expression of the gene encoding β2m or Rn18s and were quantified by the $^{\Delta\Delta}$CT method as previously described. [6]

Immunofluorescence and image quantification

NF-κB p65 immunofluorescence was performed as previously reported. [7] Peritoneal macrophages were seeded onto coverslips in 24-well plates and were stimulated with 100 ng/ml LPS for 15 min. Cells were fixed with 4% paraformaldehyde in PBS (Electron Microscopy Sciences) for 15 min at room temperature. Coverslips were incubated sequentially with 0.1% Triton-X100 (Sigma) (10 min, room temperature), blocking buffer (5% donkey serum in PBS, 60 min, room temperature), NF-κB p65 (D14E12) XP rabbit antibody (D14E12; Cell Signaling) diluted in staining buffer (1% donkey serum in PBS, overnight, 4°C) and Alexa Fluor 568-conjugated donkey anti-rabbit IgG antibody (Invitrogen) diluted in staining buffer (1 hr, room temperature). Nuclei were counterstained with 2 μg/ml of the nuclear stain Hoechst (Invitrogen) for 5 min. Coverslips were mounted on to glass slides (Fisher Scientific) by using SlowFade Gold antifade reagents (Life Technologies). Fluorescence images were captured on a Zeiss Axio Observer Z1 inverted microscope and were analyzed with Cell Scoring Application Module in MetaMorph software (Molecular Devices).

Plasma cholesterol measurements

Plasma cholesterol assay was performed using commercial kit (Wako Diagnostics) according to the manufacturer's instructions.

Histological quantification of atherosclerosis

Aortic root sections were stained and quantified as we previously described.[1, 8] Beginning at the base of the aortic root, 75 sections were cut at 10 μm, collected, and arranged in 3 sections per slide. Atherosclerotic lesions in the aortic root were quantified by staining with oil red O to reveal neutral lipids in 15 cross-sections, 20 μm apart starting at the coronary ostium and extending through the base of the aortic valve. Adjacent sections were labeled with a primary rat anti-mouse MOMA-2 antibody (Cedarlane labs, NC) and a rabbit anti-mouse Ki-67 (Abcam), detected with a chicken anti-rat IgG (H+L) antibody and a donkey anti-rabbit IgG (H+L) antibody conjugated with Alexa Fluor 594 and Alexa Fluor 488 (Life Technologies), respectively. Slides were mounted on a Zeiss AxioObserver microscope and images captured with a Retiga-SRV CCD camera equipped with RGB color filter (Qimaging, Surrey, BC, Canada). Oil red O and MOMA-2 Surface areas, and the numbers of Ki-67 positive cells were quantified with Metamorph software (Molecular Devices).

Statistical analysis

All statistical analyses were performed using GraphPad Prism 5.0 (GraphPad Software). *In vitro* experiment was carried out with three to four independent biological samples. qRT-PCR were performed in two or three technical replicates for each biological sample. Data are presented as means ± SEM. Differences between experimental groups were analyzed for statistical significance by unpaired Student's t test or by 1-way ANOVA followed by Bonferroni test for the selected pairs. A value of $P<0.05$ was considered significant.

Supplemental Figure and Figure Legends

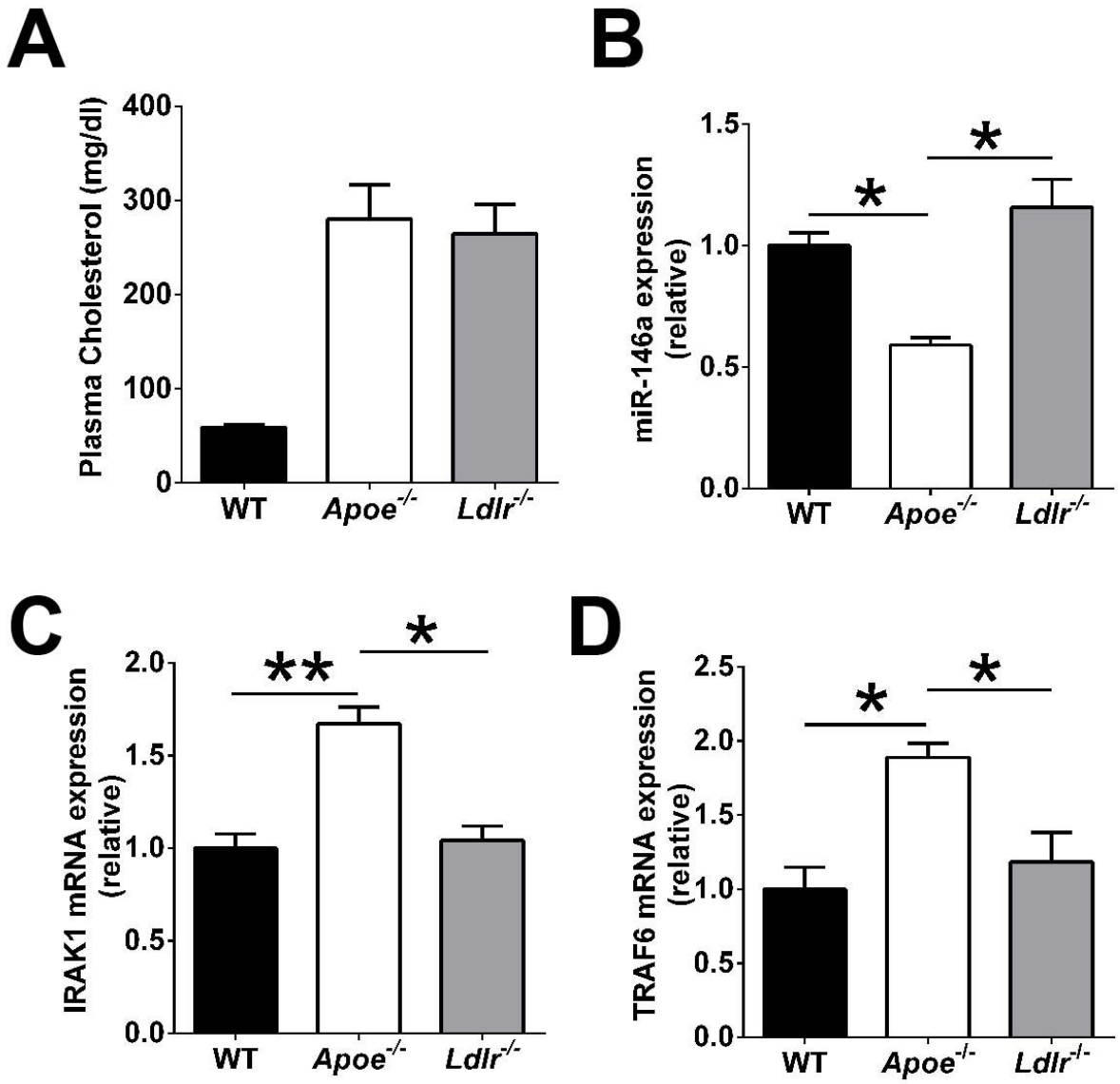

Online Figure I. MiR-146a levels and activity is reduced in macrophages derived from *Apoe*$^{-/-}$ mice, but not in those derived from *Ldlr*$^{-/-}$ mice

(A) Plasma cholesterol levels in 3~4-week-old WT, *Apoe*$^{-/-}$, and *Ldlr*$^{-/-}$ mice; (B) qPCR analysis of miR-146a levels in peritoneal macrophages derived from WT, *Apoe*$^{-/-}$, and *Ldlr*$^{-/-}$ mice; (C) mRNA levels of IRAK1 and TRAF6 in peritoneal macrophages derived from WT, *Apoe*$^{-/-}$, and *Ldlr*$^{-/-}$ mice were examined by qPCR. n=9~10 for A, n=8 for B and C. *, P<0.05; **, P<0.01.

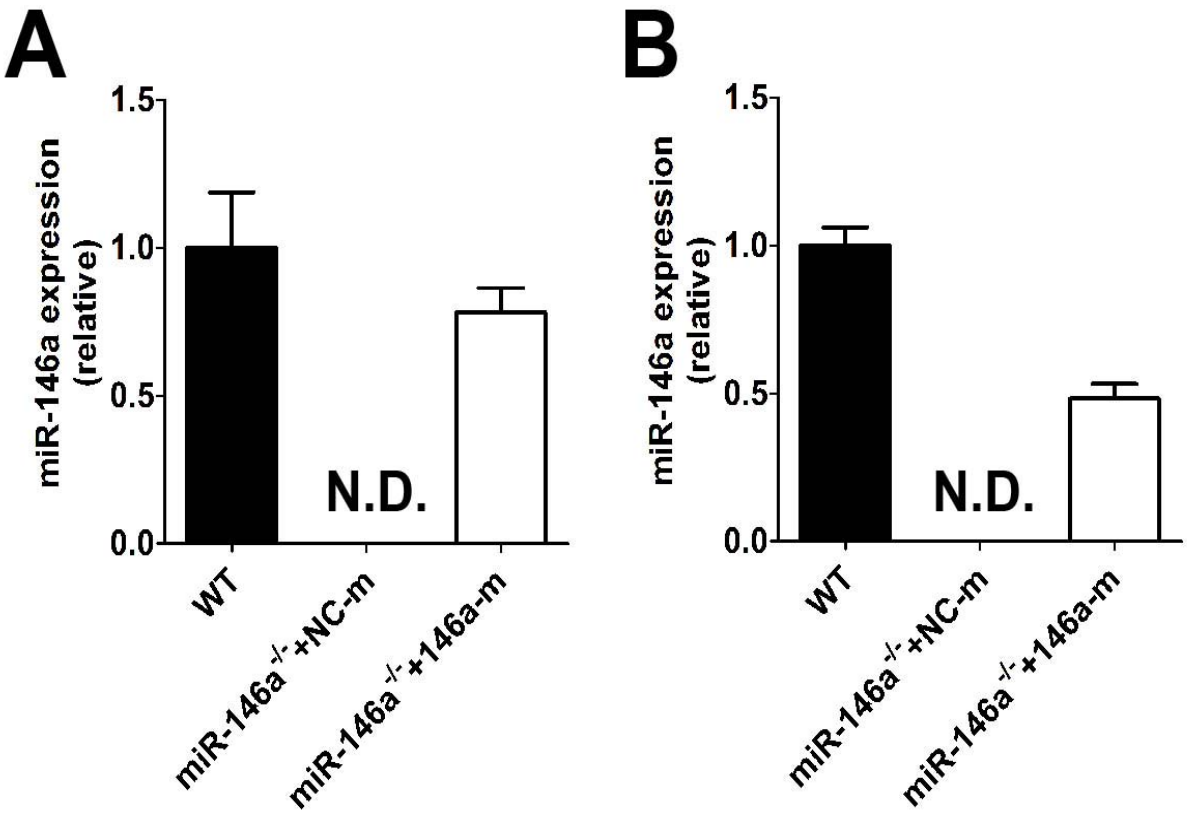

Online Figure II Validation of delivery of miR-146a mimetics into Ly-6C^{high} monocytes and macrophages *in vivo*

MiR-146$^{-/-}$ mice (n=2/group) were intravenously administered miRNA negative control mimetics (NC-m) or miR-146a mimetics (146a-m) twice a week for two weeks. Splenic Ly-6C^{high} monocytes (A) and peritoneal macrophages (B) were isolated and analyzed for miR-146a levels by qRT-PCR. The results were compared to WT mice set arbitrarily to 1. N.D., not detectable.

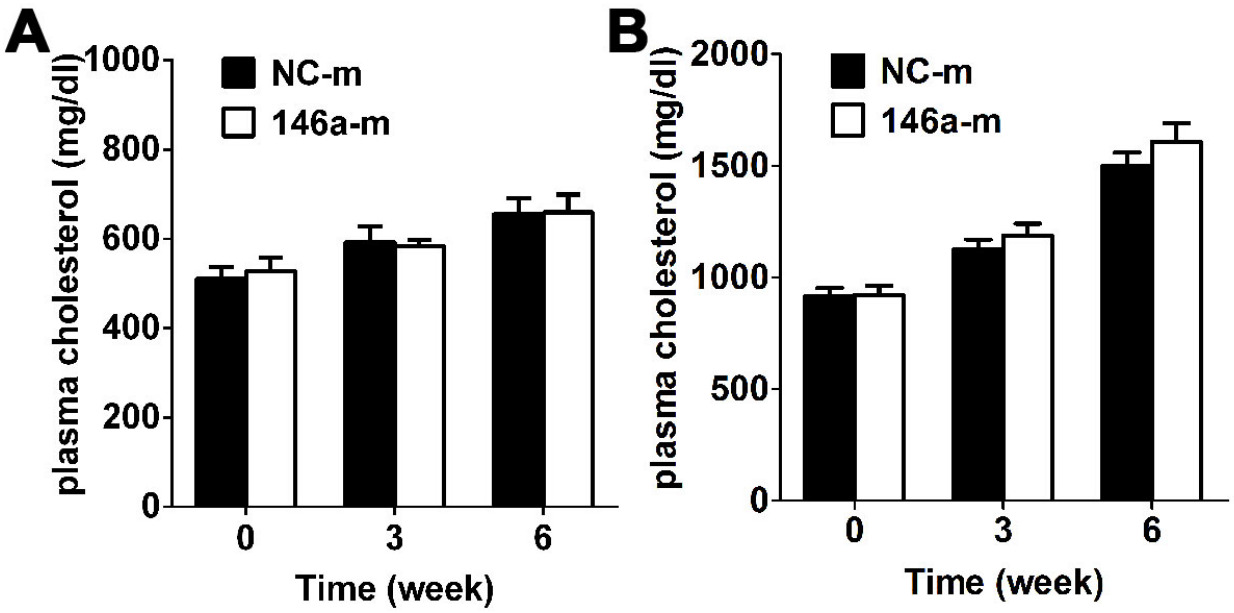

Online Figure III. Systemic delivery of miR-146a mimetics does not alter plasma cholesterol levels in *Apoe*$^{-/-}$*Ldlr*$^{-/-}$ mice fed a chow diet, or *Ldlr*$^{-/-}$ mice fed a high fat diet
Cohorts of ~10-week old *Apoe*$^{-/-}$*Ldlr*$^{-/-}$ mice (n=9~12/group) receiving a chow diet or *Ldlr*$^{-/-}$ mice (n=9/group) fed a high fat diet were intravenously administered miRNA negative control mimetics (NC-m) or miR-146a mimetics (146a-m) twice a week. Blood was collected before, 3 weeks and 6 weeks after initiation of the treatment and plasma cholesterol levels were determined by enzymatic assay. **A**, *Apoe*$^{-/-}$*Ldlr*$^{-/-}$ mice; **B**, *Ldlr*$^{-/-}$ mice; Data are shown as the means ± SEM.

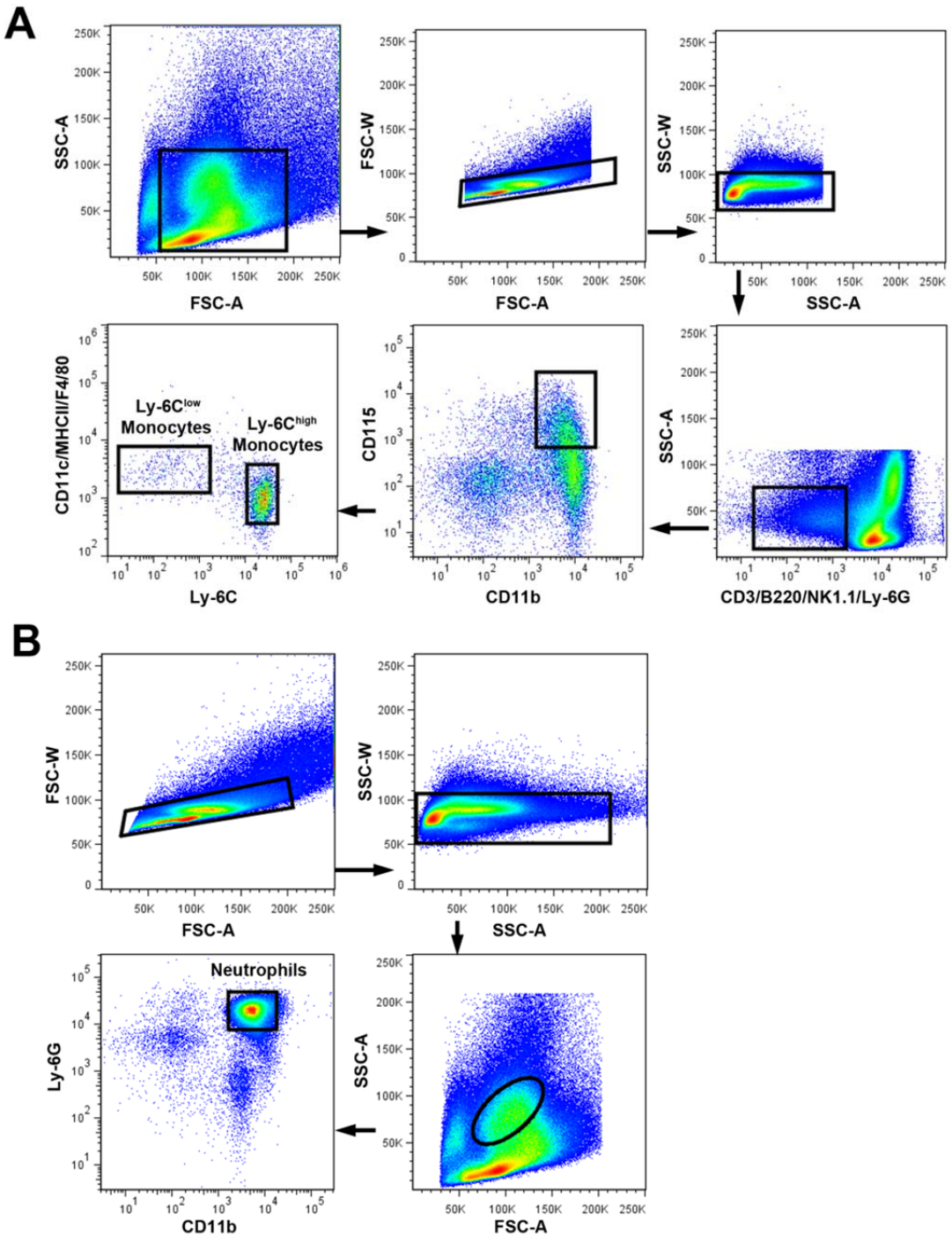

Online Figure IV. Gating strategy for the isolation of Ly-6C^{high}, Ly-6C^{low} monocytes and neutrophils from mouse bone marrow

A, Monocytes were identified as (CD3 B220 NK1.1)$^{-}$CD11b^{+} CD115^{high} (CD11c MHCII F4/80)^{low}. Monocytes were then subdivided based on Ly-6C expression. **B,** Neutrophils were identified as SSC^{high}CD11b^{+}Ly6G^{+}.

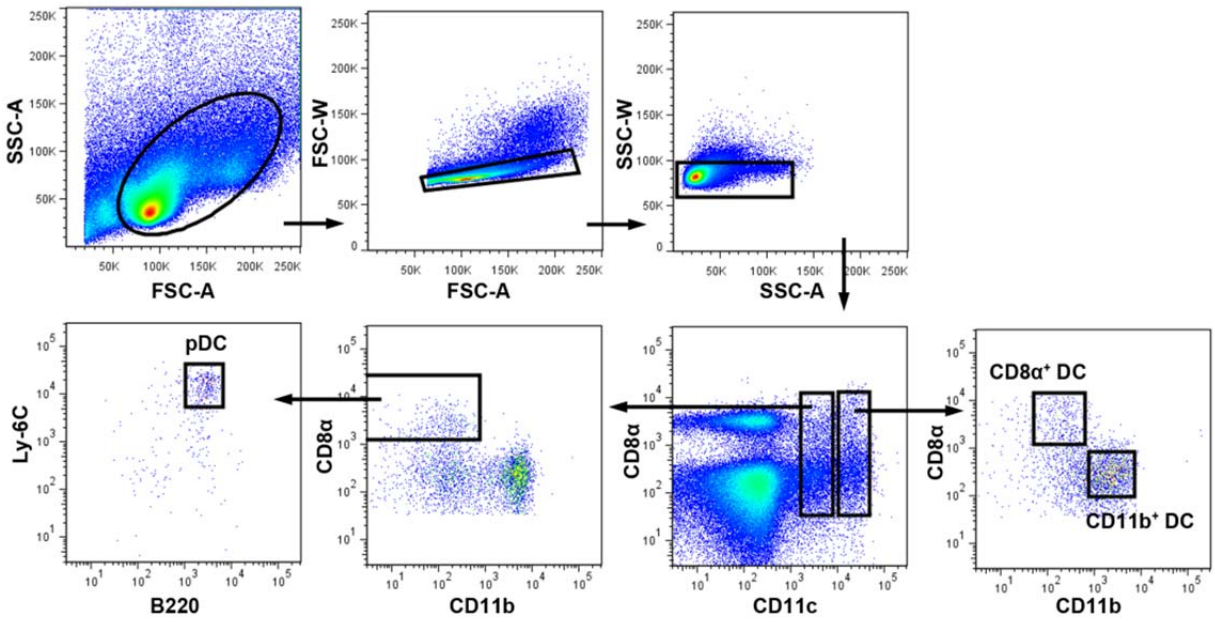

Online Figure V. Gating strategy for the isolation of splenic DC subsets and pDC
$CD8\alpha^+$ DC was defined as $CD11C^{high}CD8\alpha^+$; $CD11b^+$ DC was defined as $CD11c^{high}CD11b^+$. pDC were identified as $CD11c^{int}CD11b^-B220^+Ly\text{-}6C^+$. Int, intermediate.

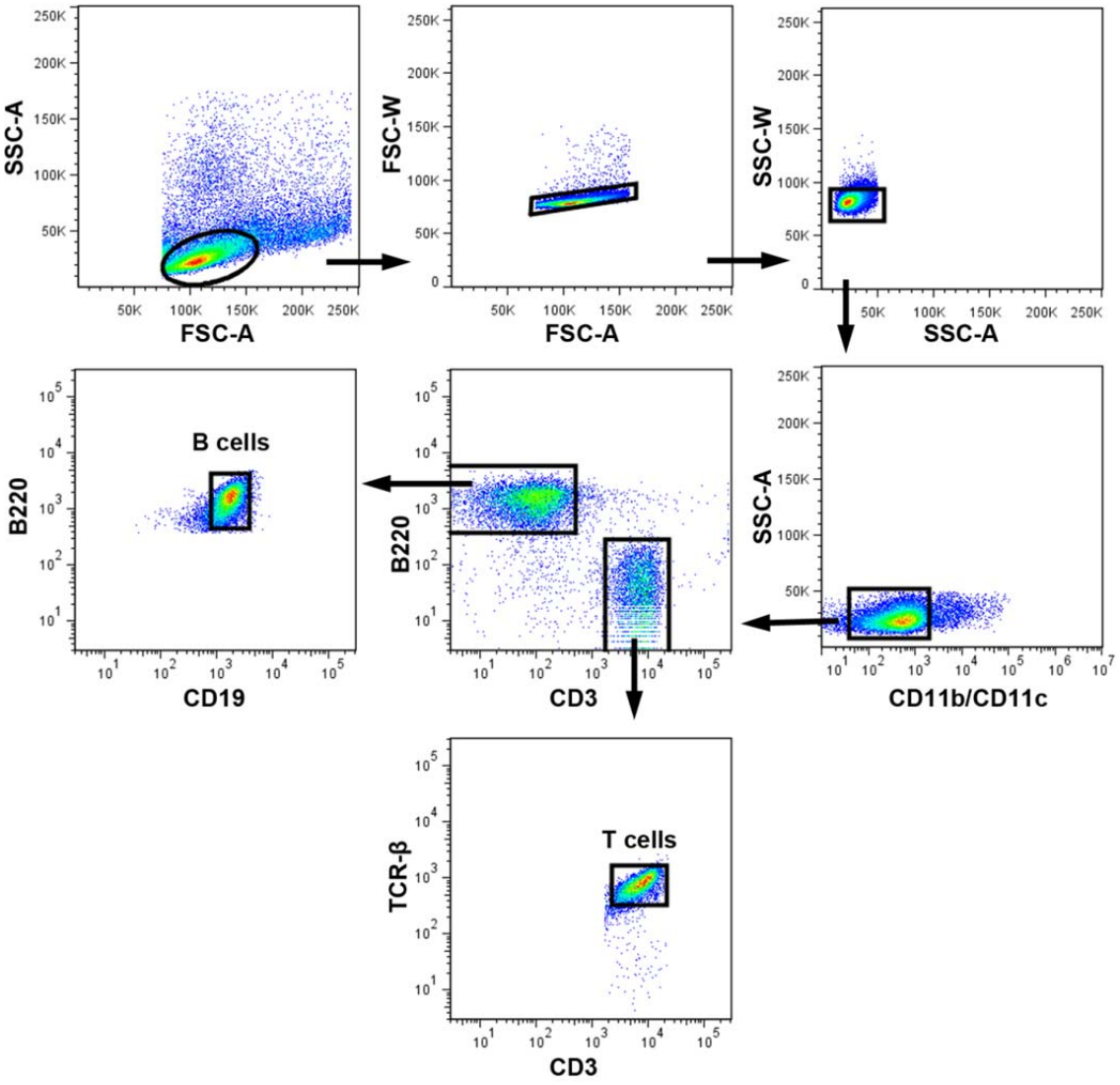

Online Figure VI. Gating strategy for B cell and T cells in mouse spleen
B cells were defined as $B220^{+}$ $CD19^{+}$; T cells were defined as $CD3^{+}$ TCR-β^{+}.

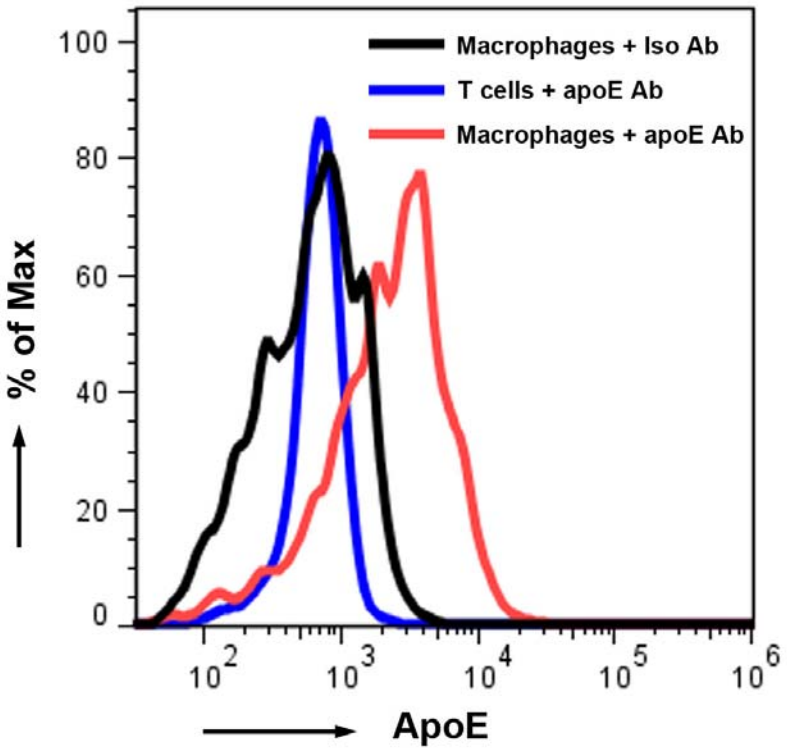

Online Figure VII. Validation of apoE antibody for intracellular flow cytometry
Peritoneal macrophages were isolated from WT mice and incubated with antibodies against CD11b, F4/80, and TCR-β. After fixation and permeabilization, the cells were stained with an isotype antibody (Iso Ab) or an anti-apoE antibody (apoE Ab). Histograms of apoE expression in gated $CD11b^{+}F4/80^{high}$ macrophages and $CD11b^{-}TCR\text{-}\beta^{+}$ were shown. Ab, antibody.

Supplemental References

1. Gaudreault N, Kumar N, Posada JM, Stephens KB, Reyes de Mochel NS, Eberle D, Olivas VR, Kim RY, Harms MJ, Johnson S, Messina LM, Rapp JH, Raffai RL. ApoE suppresses atherosclerosis by reducing lipid accumulation in circulating monocytes and the expression of inflammatory molecules on monocytes and vascular endothelium. *Arterioscler Thromb Vasc Biol*. 2012;32:264-272
2. Choi JH, Cheong C, Dandamudi DB, Park CG, Rodriguez A, Mehandru S, Velinzon K, Jung IH, Yoo JY, Oh GT, Steinman RM. Flt3 signaling-dependent dendritic cells protect against atherosclerosis. *Immunity*. 2011;35:819-831
3. Crotti A, Benner C, Kerman BE, Gosselin D, Lagier-Tourenne C, Zuccato C, Cattaneo E, Gage FH, Cleveland DW, Glass CK. Mutant Huntingtin promotes autonomous microglia activation via myeloid lineage-determining factors. *Nat Neurosci*. 2014;17:513-521
4. Pourcet B, Feig JE, Vengrenyuk Y, Hobbs AJ, Kepka-Lenhart D, Garabedian MJ, Morris SM, Jr., Fisher EA, Pineda-Torra I. LXRalpha regulates macrophage arginase 1 through PU.1 and interferon regulatory factor 8. *Circ Res*. 2011;109:492-501
5. Etzrodt M, Cortez-Retamozo V, Newton A, Zhao J, Ng A, Wildgruber M, Romero P, Wurdinger T, Xavier R, Geissmann F, Meylan E, Nahrendorf M, Swirski FK, Baltimore D,

Weissleder R, Pittet MJ. Regulation of monocyte functional heterogeneity by miR-146a and Relb. *Cell Rep*. 2012;1:317-324
6. Li K, Xu W, Guo Q, Jiang Z, Wang P, Yue Y, Xiong S. Differential macrophage polarization in male and female BALB/c mice infected with coxsackievirus B3 defines susceptibility to viral myocarditis. *Circ Res*. 2009;105:353-364
7. Schneider M, Zimmermann AG, Roberts RA, Zhang L, Swanson KV, Wen H, Davis BK, Allen IC, Holl EK, Ye Z, Rahman AH, Conti BJ, Eitas TK, Koller BH, Ting JP. The innate immune sensor NLRC3 attenuates Toll-like receptor signaling via modification of the signaling adaptor TRAF6 and transcription factor NF-kappaB. *Nat Immunol*. 2012;13:823-831
8. Gaudreault N, Kumar N, Olivas VR, Eberle D, Stephens K, Raffai RL. Hyperglycemia impairs atherosclerosis regression in mice. *Am J Pathol*. 2013;183:1981-1992